Supporting Information

A General Protocol for Addressing Speciation of the Active Catalyst Applied to Ligand-Accelerated Enantioselective C(sp^3)-H Bond Arylation

David E. Hill,[1] Qing-lan Pei,[2] En-xuan Zhang,[2] James R. Gage,[2] Jin-Quan Yu,[1] and Donna G. Blackmond[1*]

[1]Department of Chemistry, The Scripps Research Institute, La Jolla, California 92037 USA; [2]New Technology Development Laboratory, Asymchem, Inc., 7 Binhai Xinqu, Tianjin, CN 300457

Correspondence to: Blackmond@scripps.edu

Table of Contents

1. General Remarks……..……...……S2
2. Ligands/Substrate…...……..……...…....S3
3. Kinetics Experiments…….…....S4
4. Nonlinear Effect..……..……....S10
5. Kinetic Modeling ……...…..……..…….……..S11
6. Gas Chromatography with Flame Ionization Detection…….…….……...S13
7. HPLC on Chiral Stationary Phase ……..S15
8. References……..…S20

1. **General Remarks**

Materials: Silver carbonate was purchased from Sigma Aldrich. Ethyl acetate, hexanes, and acetone were purchased from Fischer Scientific. Chloroform-d_1 (99.8% D) was purchased from Cambridge Isotope Laboratories, Inc. Helium (99.999%), hydrogen, and extra dry air were purchased from Praxair. Palladium acetate and 1,1,1,3,3,3-hexafluoro-2-propanol (HFIP) were purchased from Oakwood Chemical. 4-iodoanisole was purchased from Acros Organics. Silica gel 60, 0.032-0.063 mm (230-450 mesh), was purchased from Alfa Aesar. Magnesium sulfate and Silica gel 60 F_{254} plates (20 x 20 cm) were purchased from EMD.

Analysis: Gas chromatography measurements were acquired with an Agilent Technologies 7890A gas chromatography (USA) equipped with a flame ionization detector and with a DB-5 column (polyimide coating, 30 m 0.25 mm x 0.25 μm) manufactured by J&W. Enantiomeric excess (*e.e.*) was determined using an Agilent Technologies 1200 Series HPLC.

2. **Ligands/Substrate**

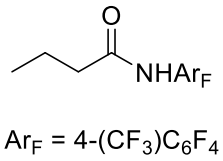

1

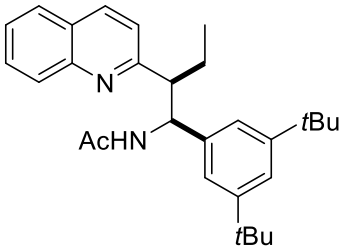

4

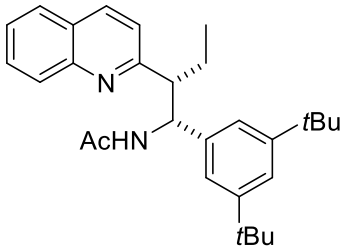

4-ent

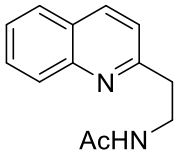

5

1, **4**, **4**-ent, and **5** were prepared according to literature procedure.[1]

3. **Kinetics Experiments**

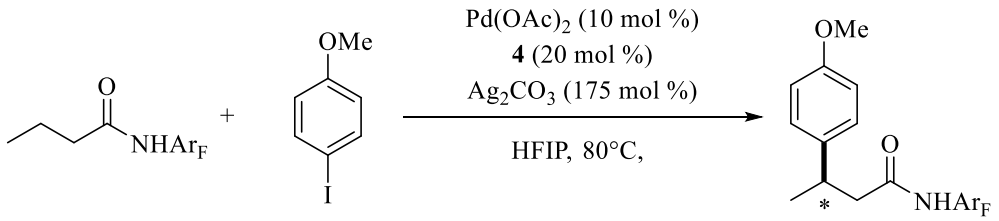

1 (0.1 M) **2** (0.25 M) **3**

Ar_F = 4-$(CF_3)C_6F_4$

3.1. General kinetics procedure.

To a 5 mL volumetric flask with palladium acetate (15.0 mg, 0.067 mmol), **4**-ent (57.4 mg, 0.133 mmol), and decafluorobiphenyl (111.4 mg, 0.333 mmol) was added HFIP. The contents of the 5 mL volumetric were homogenized with sonication and then diluted with HFIP to prepare a 5 mL palladium acetate/**4**-ent/decafluorobiphenyl stock solution (0.013 M, 0.027 M, 0.067 M respectively). To a 1 dram vial with screw cap teflon septum, stir bar, **1** (30.3mg, 0.100 mmol), and **2** (58.5mg, 0.250 mmol) was added palladium acetate/**4**-ent/decafluorobiphenyl stock solution (750 µL) and HFIP (250 µL). The contents of the vial were homogenized by heating and stirring at 82 °C for 15 seconds. The 1 dram vial was removed from heat and then immediately cooled in an ambient temperature water bath. To the ambient temperature 1 dram vial was added silver carbonate (48.3 mg, 0.175 mmol). The 1 dram vial was sealed and then shaken by hand several times. Immediately after shaking by hand, the cap of the 1 dram vial was removed, an aliquot (~15 μL) of the mixture was taken using a new plastic syringe (1 mL) and new needle, and then the capped 1 dram vial was placed in a heating block at 82 °C. The aliquot was quenched with ethyl acetate (1 mL), filtered with a syringe filter (PTFE, 0.45 μm), and then analyzed by gas chromatography with a flame ionization detector (GC-FID). For additional time points, the vial was removed from heat, cooled in an ambient temperature water bath for 10 seconds, uncapped, sampled (~15 μL), and then the capped vial was placed back in the heating block at 82 °C.

3.2. Kinetics Experiments at Same Excess

Experiments at same excess were designed using Reaction Progress Kinetic Analysis protocols [3,4] and were conducted as described by the general kinetics procedure except with the following changes designated in Table S1.

Table S1: Conditions for A, B, and C: [$Pd(OAc)_2$] = 0.01 M, [**4**-ent] = 0.02 M, and [decafluorobiphenyl] = 0.05 M. For vial C, solid **3** was added to the vial with **1** prior to adding any stock solutions, and 250 µL of an anisole stock solution in HFIP (2.6 mg in 3 mL, 0.008 M) was added.

Experiment	[**1**] (M)	[**2**] (M)	Ag_2CO_3 (mg)	[**3**] (M)	[anisole] (M)
3.2 A	0.090	0.210	48.5	0	0
3.2 B	0.070	0.194	42.9	0	0
3.2 C	0.075	0.196	42.5	0.002	0.017

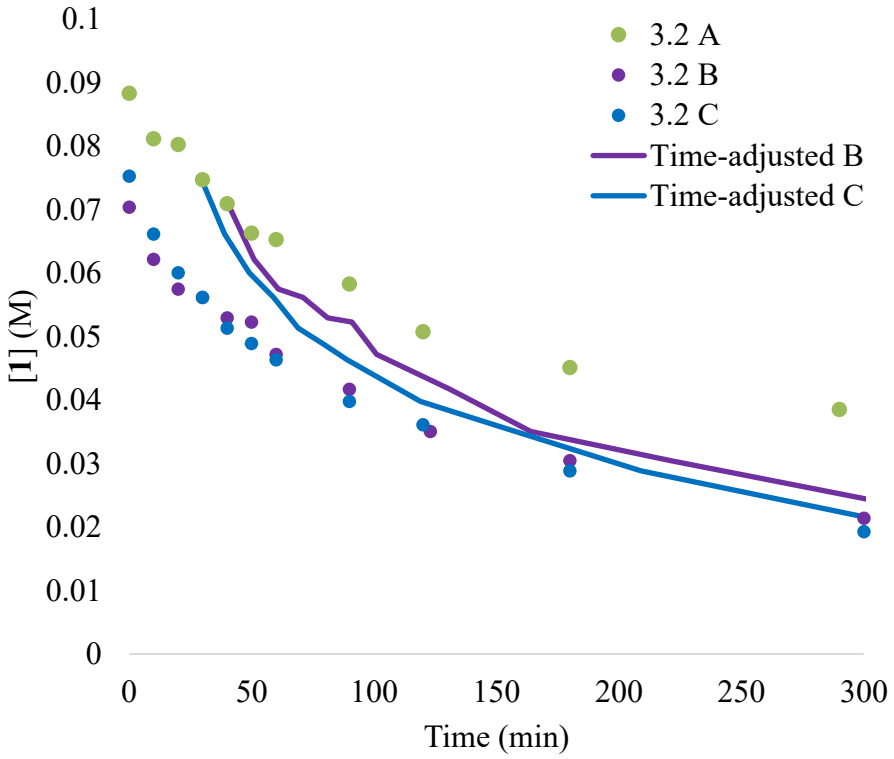

Figure S1: Kinetic profile for experiments performed at the same excess (3.2).

3.3. Kinetics Experiments at Different Excess

Experiments at different excess were designed using Reaction Progress Kinetic Analysis protocols [3,4] and were conducted as described by the general kinetics procedure except with the following changes designated in Table S2.

Table S2: Conditions for A, B, C, and D: [$Pd(OAc)_2$] = 0.01 M, [**4**-ent] = 0.02 M, and [decafluorobiphenyl] = 0.05 M.

Experiment	[**1**] (M)	[**2**] (M)	Ag_2CO_3 (mg)
3.3 A	0.090	0.215	48.9
3.3 B	0.091	0.432	48.7
3.3 C	0.090	0.099	48.1
3.3 D	0.186	0.213	48.6

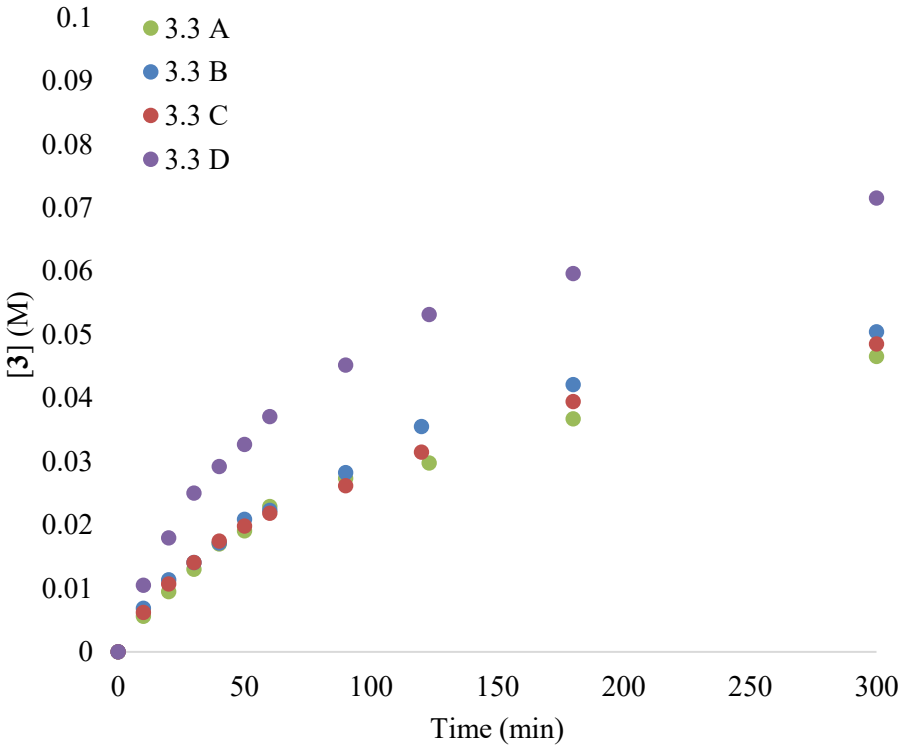

Figure S2: Kinetic profiles for experiments performed at different excess (3.3).

Rate (mM/min) data for 3.3 are plotted in Figure 1 of main paper.

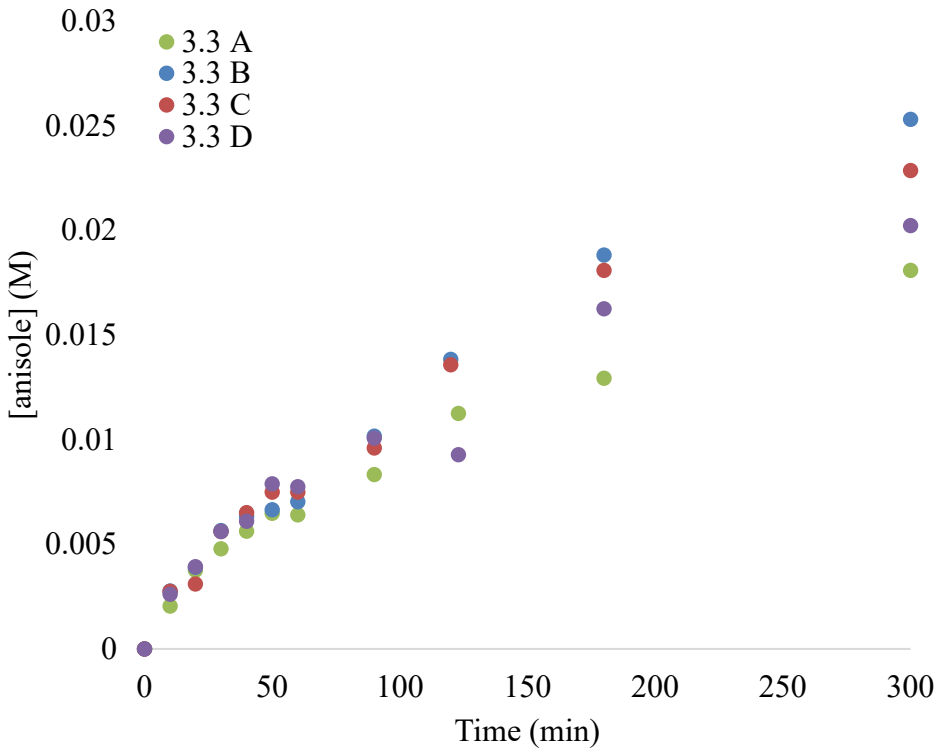

Figure S3: Kinetic profile of dehalogenation of **2** for experiments performed at different excess (3.3).

3.4. Order in Catalyst

3.4.1. Order in catalyst using **4**-ent

Experiments were conducted as described by the general kinetics procedure except with the following changes designated in Table S3.

Table S3: Conditions for A and B: $Pd(OAc)_2$: **4**-ent = 1:2, [decafluorobiphenyl] = 0.05 M, and a total reaction volume of 1.2 mL.

Experiment	[**1**] (M)	[**2**] (M)	[$Pd(OAc)_2$] (M)	Ag_2CO_3 (mg)
3.4.1 A	0.091	0.218	0.01	57.9
3.4.1 B	0.089	0.219	0.02	58.5

3.4.2. Order in catalyst using **5**

Experiments were conducted as described by the general kinetics procedure except with the following changes designated in Table S4.

Table S4: Conditions for A, B, and C: $Pd(OAc)_2$: **5** = 1:2, [decafluorobiphenyl] = 0.05 M, and a total reaction volume of 0.6 mL.

Experiment	[**1**] (M)	[**2**] (M)	[$Pd(OAc)_2$] (M)	Ag_2CO_3 (mg)
3.4.2 A	0.099	0.218	0.01	29.0
3.4.2 B	0.096	0.206	0.02	29.2
3.4.2 C	0.100	0.203	0.03	29.8

3.5. Burés Variable Time Normalization Analysis (VTNA).

A method to determine a "power-law" reaction order in catalyst concentration was recently published by Burés.[2] The mathematical details are given in that publication. Briefly, reactant or product concentration profiles are monitored carried out using different starting concentrations of catalyst. The data are plotted with product concentration on the y-axis and with the x-axis normalized as [**catalyst**]^n * time, where [**catalyst**] is the initial catalyst concentration under examination and n is the order in [**catalyst**]. This normalization will result in overlay between the profiles from different catalyst concentrations when the order n is correctly selected. Table S5 and Table S6 list the results of applying Burés Variable Time Normalization Analysis to experiments from 3.4.

Table S5: [**3**] over time for reactions using **4**-ent based catalyst in 3.4.1 A and 3.4.1 B. Burés VTNA analysis applied to 3.4.1 A and 3.4.1 B.

	3.4.1 A		3.4.1 B	
Time (min)	[**3**] (M)	$Time * [0.01]^1$	[**3**] (M)	$Time * [0.02]^1$
0	0.000	0.000	0.000	0.000
10	0.013	0.098	0.023	0.195
30	0.032	0.293	0.052	0.586
60	0.049	0.586		

Table S6: [**3**] over time for reactions using **5** based catalyst in 3.4.2 A, 3.4.2 B, and 3.4.2 C. Burés VTNA analysis applied to 3.4.2 A, 3.4.2 B, and 3.4.2 C.

	3.4.2 A		3.4.2 B		3.4.2 C	
Time (hr)	[**3**] (M)	$Time * [0.01]^{0.5}$	[**3**] (M)	$Time * [0.02]^{0.5}$	[**3**] (M)	$Time * [0.03]^{0.5}$
0	0.000	0.0	0.000	0.0	0.000	0.0
1	0.004	0.1	0.007	0.1	0.006	0.2
1.8	0.007	0.2	0.010	0.3	0.009	0.3
3	0.011	0.3	0.015	0.4	0.015	0.5
4	0.013	0.4	0.019	0.6	0.018	0.7
5	0.016	0.5	0.021	0.7		
6	0.017	0.6				

The results from the Burés VTNA analysis in Table S5 and Table S6 are plotted Figure 2 of main paper.

The reaction progress for 3.4.1 was significantly faster than it was for 3.4.2, so the two experiments are normalized using two different units of time to fit both data sets on the same abscissa. The data from 3.4.1 are normalized using time in minutes, and the data from 3.4.2 are normalized using time in hours.

4. **Nonlinear Effect**

Experiments were conducted as described by the general kinetics procedure except with the following changes described in Table S7.

Table S7: Conditions for nonlinear effect experiments: $[Pd(OAc)_2]$ = 0.01 M. Reactions were run for 6 hours, quenched with ethyl acetate, and chromatographed to isolate product in accordance with literature precedent.[1]

Experiment	Enantiomeric Excess of Ligand (% *e. e.*)	[**1**] (M)	[**2**] (M)	Ag_2CO_3 (mg)	[**4**] (M)	[**4**-ent] (M)
A	100	0.100	0.250	77.8	0.0120	0
B	60	0.101	0.251	77.5	0.0096	0.0024
C	40	0.101	0.249	76.5	0.0084	0.0036
D	20	0.101	0.251	77.4	0.0072	0.0048
E	0	0.099	0.249	78	0.0060	0.006
F	-20	0.101	0.249	76.7	0.0048	0.0072
G	-40	0.100	0.251	77	0.0036	0.0084
H	-60	0.101	0.250	77.8	0.0024	0.0096
I	-100	0.099	0.252	77.6	0.0000	0.012

Ligand enantiomeric excess vs product enantiomeric excess data plotted in Figure 4 of main paper.

5. **Kinetic Modeling**

5.1. Kinetic Modeling of Monomer-Dimer Catalyst Behavior

For the case where achiral Pd catalysts form dimers, the monomer-dimer equilibrium is given by eq 1 from the text:

$$PdL + PdL \overset{K_{eq}}{\rightleftharpoons} D \qquad \left[D\right] = K_{eq}\left[PdL\right]^2$$

The total Pd concentration $[Pd]_{total}$ is given by:

$$\left[Pd\right]_{total} = \left[PdL\right] + 2\cdot\left[D\right] = \left[PdL\right] + 2\cdot K_{eq}\left[PdL\right]^2$$

We solve for $[PdL]$ using the quadratic formula:

$$2\cdot K_{eq}\left[PdL\right]^2 + \left[PdL\right] - \left[Pd\right]_{total} = 0$$

$$a = 2\cdot K_{eq}$$

$$b = 1$$

$$c = -\left[Pd\right]_{total}$$

$$\left[PdL\right] = \frac{-1 + \sqrt{1 + 8K_{eq}\left[Pd\right]_{total}}}{4K_{eq}}$$

Using these relationships, we can plot $[PdL]$ and $[D]$ vs. $[Pd]_{total}$ over any given range of catalyst concentrations and then fit this plot to a power law form for both $[PdL]^n$ and $[D]^{n'}$ to determine the observed order in catalyst for the case of K_{eq}=100 M^{-1} and $[Pd]_{total}$ from 2.5-10 mM, where monomers are the catalyst (order = n) and the case where dimers are the catalyst (order = n').

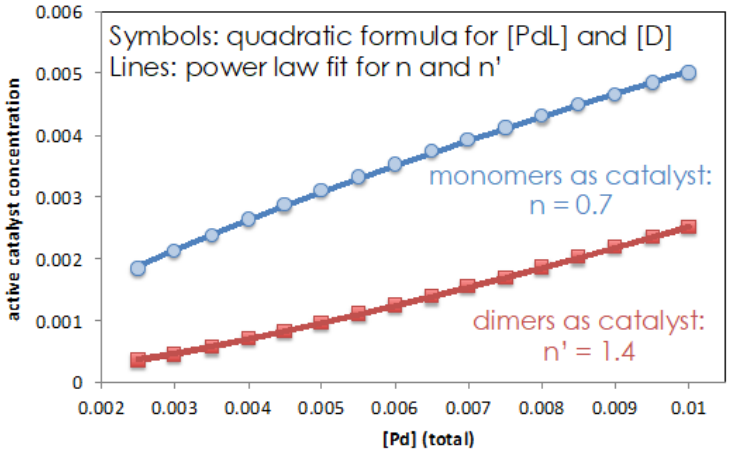

Figure S4: Active catalyst monomer/dimer speciation as a function of $[Pd]_{total}$.

A reaction exhibiting first order kinetics in substrate [A] was simulated using either monomer PdL or dimer D as catalyst, with K_{eq}=100 M^{-1} over the same range of $[Pd]_{total}$ using Copasi software:[5]

$$A + PdL \longrightarrow B + PdL$$

$$A + D \longrightarrow B + D$$

The kinetic profiles may be plotted as normalized [A] vs time and vs. time*$[cat]^n$ (using the Burés VTNA analysis[3]) as shown in Figure 3 in the text.

5.2. Kinetic Modeling of Nonenantiopure Monomer-Dimer Catalysts

For the case where chiral Pd catalysts form dimers, the monomer-dimer equilibrium for homochiral and heterochiral species are given by eqs 2-4 from the text:

$$PdL_R + PdL_R \overset{K_{homo}}{\rightleftarrows} D_{RR}$$

$$PdL_S + PdL_S \overset{K_{homo}}{\rightleftarrows} D_{SS}$$

$$PdL_R + PdL_S \overset{K_{hetero}}{\rightleftarrows} D_{RS}$$

The relative concentrations of each monomer and dimer species at equilibrium may be determined for any total Pd concentration and any values of K_{homo} and K_{hetero} by simulations of these equations using the Copasi software.[5]

6. **Gas Chromatography with Flame Ionization Detection**

For gas chromatography-flame ionization detection analysis, helium was used as the carrier gas, with a constant flow rate of 6.0 mL/min. The optimized temperature program started from 100 °C, was raised to 220 °C at a rate of 14 °C/min, then was raised to 280 °C at 12 °C/min, and then was held at 280 °C for one minute. The temperature of the detector and injector were held at 350 °C and 350 °C respectively. The retention time for each compound of interest is listed below.

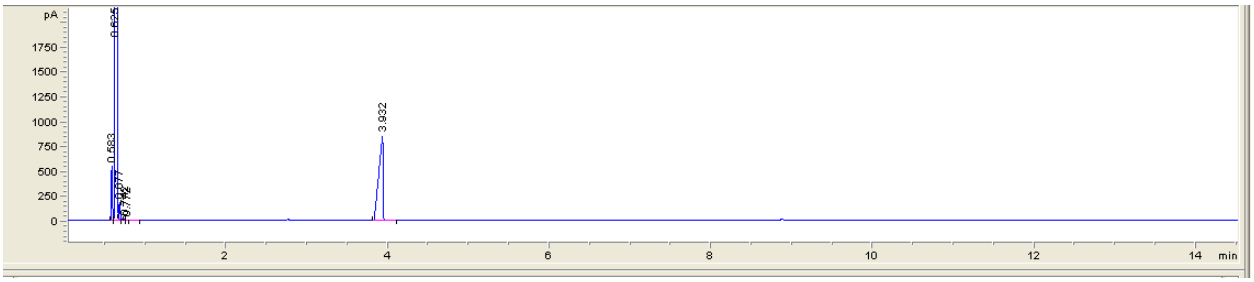

Figure S5: GC-FID of **1** with t_R = 3.93 min.

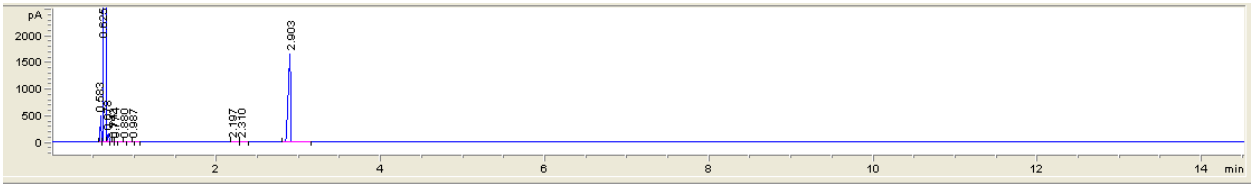

Figure S6: GC-FID of **2** with t_R = 2.90 min.

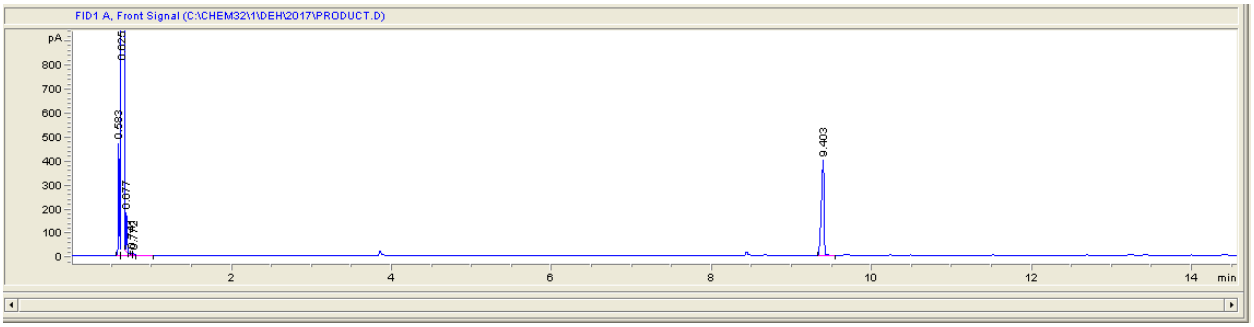

Figure S7: GC-FID of **3** with t_R = 9.40 min.

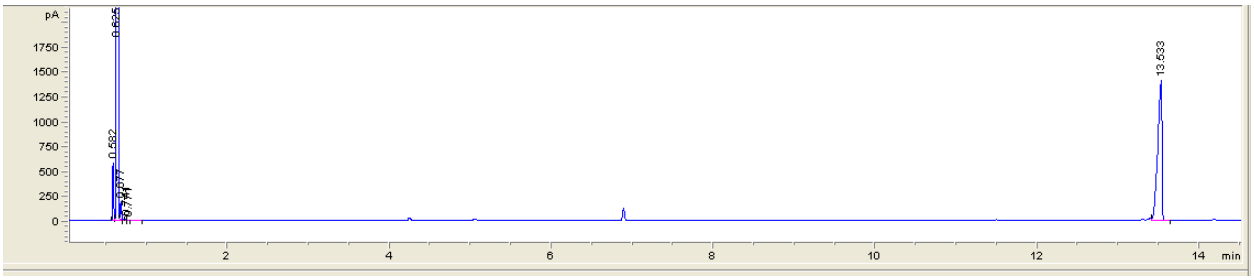

Figure S8: GC-FID of **4** with t_R = 13.53 min.

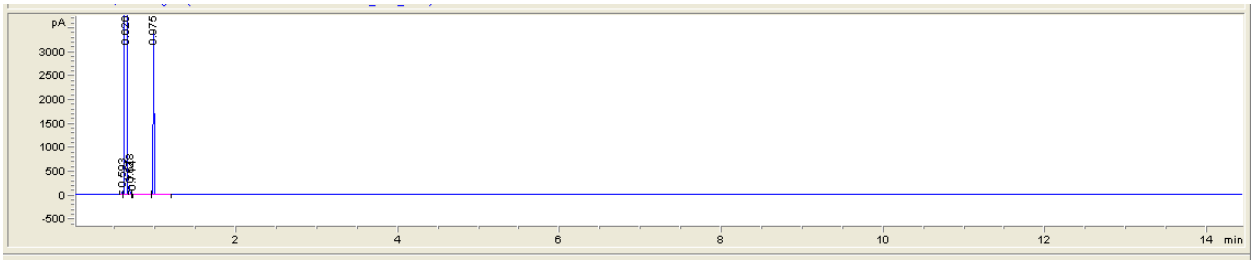

Figure S9: GC-FID of anisole with t_R = 0.98 min**.**

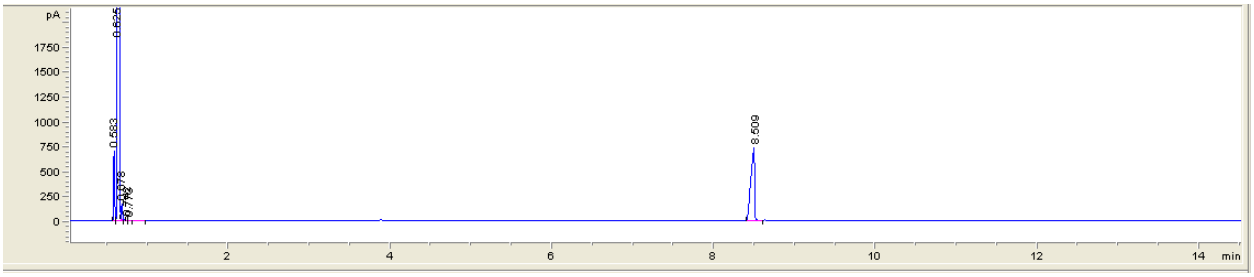

Figure S10: GC-FID of **5** with t_R = 8.50 min.

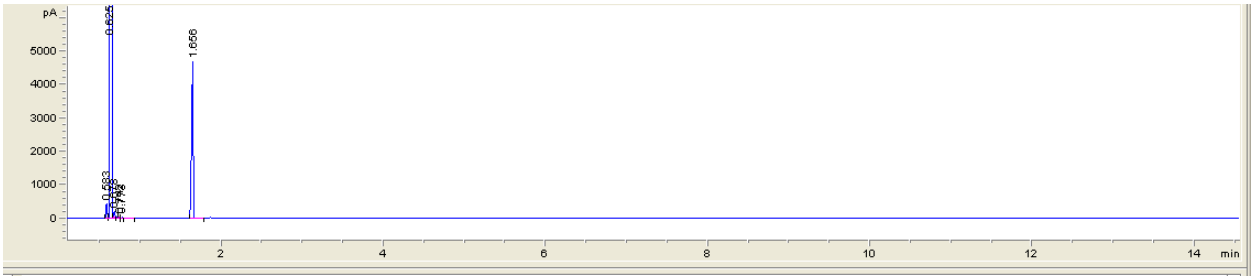

Figure S11: GC-FID of decafluorobiphenyl with t_R = 1.67 min.

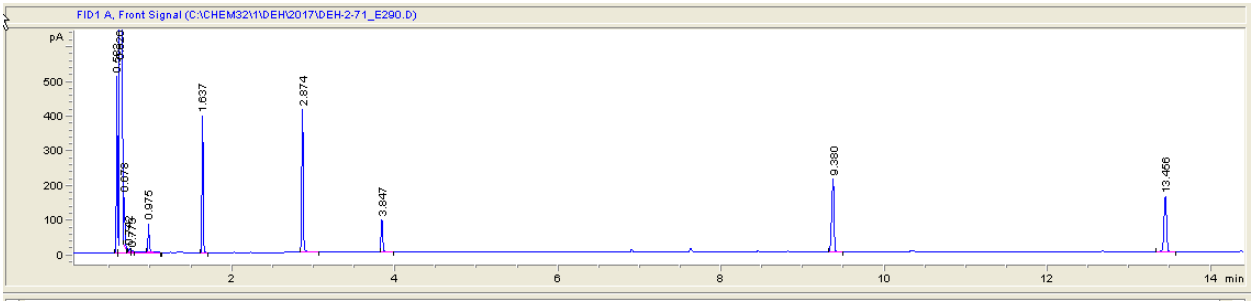

Figure S12: GC-FID of a running reaction as described in the general kinetics experimental procedure.

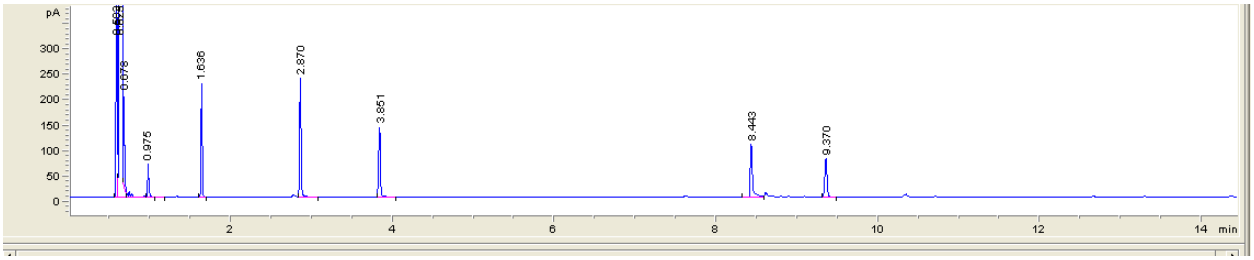

Figure S13: GC-FID of a running reaction as described in 3.4.2.

7. **HPLC on Chiral Stationary Phase**

7.1. Enantiomeric Excess measurements of for nonlinear effect experiment (4)

The enantiomeric excess of **3** was analyzed by normal phase chiral HPLC on a Daicel Group CHIRALPAK AY-H column (5 mμ, 4.6 x 250 mm) under isocratic conditions [95% hexanes / 5% ethanol (1% Trifluoroacetic acid + 1% Diethylamine), 1.0 mL/min] at 25 °C. The enantiomers were detected by UV light (210 nm).

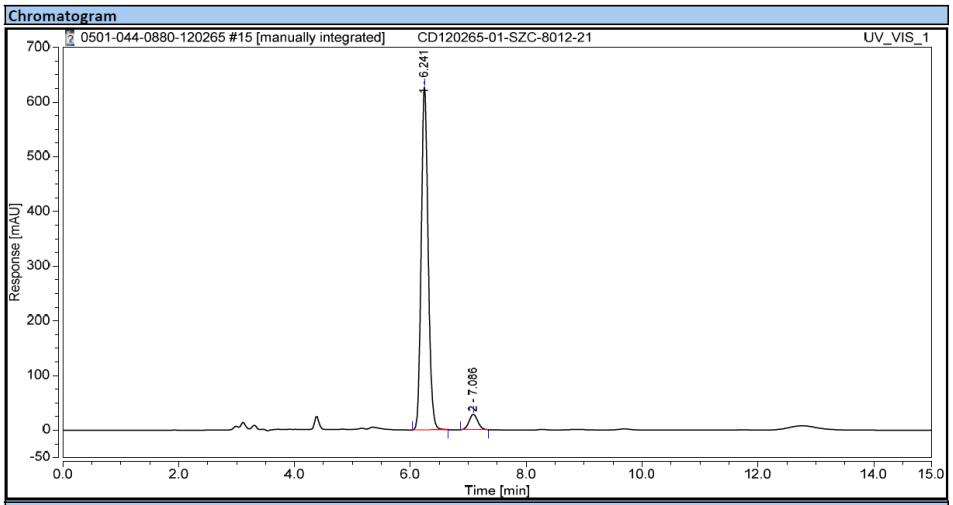

Integration Results

No.	Peak Name	Retention Time min	Area mAU*min	Height mAU	Relative Area %	Amount n.a.	Plates (EP)
1		6.241	86.700	627.223	94.6566	n.a.	13372
2		7.086	4.894	28.241	5.3434	n.a.	10619
Total:			**91.594**	**655.464**	**100.00**		

Figure S14: HPLC on chiral stationary phase for 4.A.

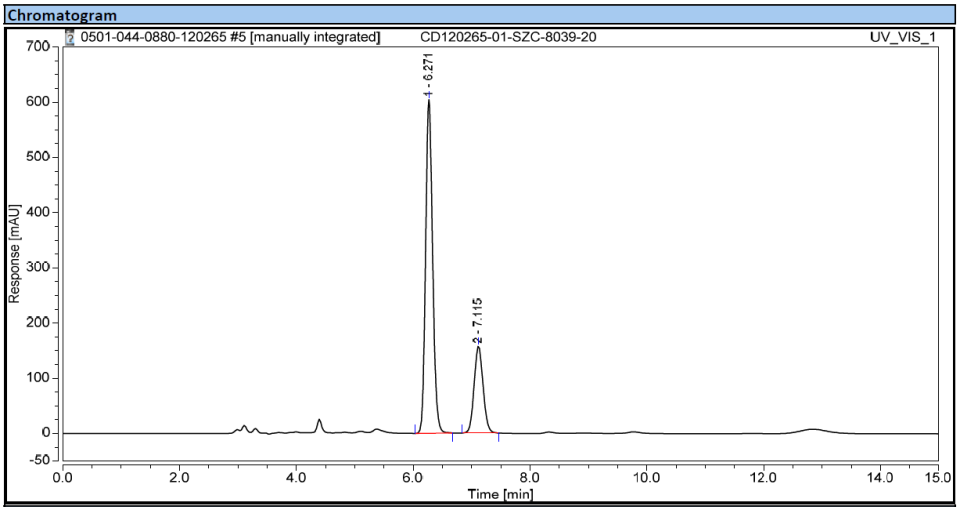

Integration Results

No.	Peak Name	Retention Time min	Area mAU*min	Height mAU	Relative Area %	Amount n.a.	Plates (EP)
1		6.271	83.881	604.383	75.0863	n.a.	13396
2		7.115	27.832	157.896	24.9137	n.a.	10536
Total:			**111.713**	**762.280**	**100.00**		

Figure S15: HPLC on chiral stationary phase for 4.B.

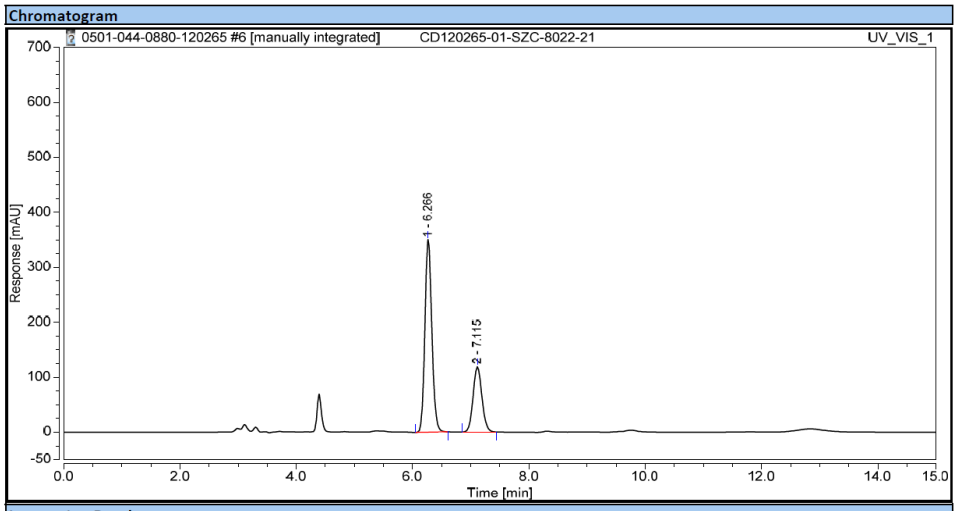

Integration Results

No.	Peak Name	Retention Time min	Area mAU*min	Height mAU	Relative Area %	Amount n.a.	Plates (EP)
1		6.266	48.464	350.369	69.9343	n.a.	13454
2		7.115	20.835	118.713	30.0657	n.a.	10578
Total:			**69.299**	**469.082**	**100.00**		

Figure S16: HPLC on chiral stationary phase for 4.C.

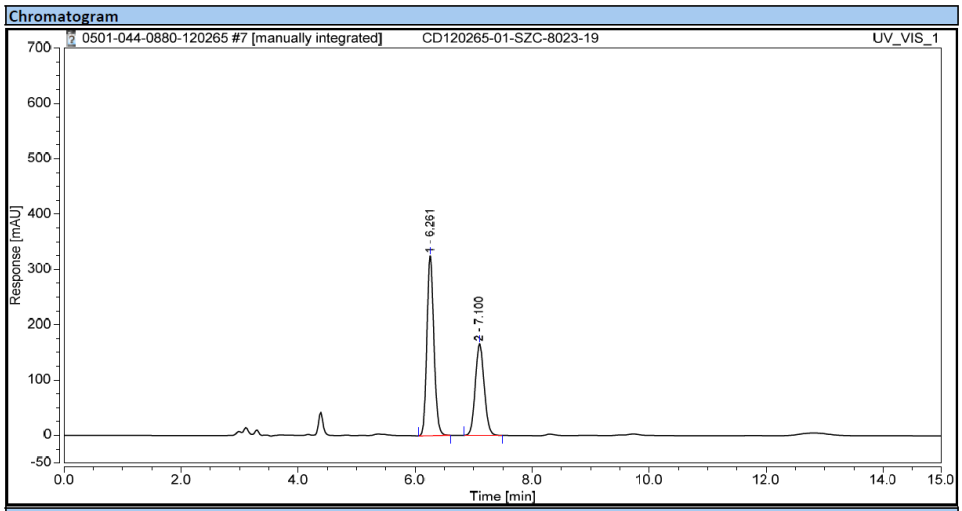

Integration Results

No.	Peak Name	Retention Time min	Area mAU*min	Height mAU	Relative Area %	Amount n.a.	Plates (EP)
1		6.261	44.871	324.913	60.6547	n.a.	13439
2		7.100	29.107	165.512	39.3453	n.a.	10528
Total:			**73.978**	**490.425**	**100.00**		

Figure S17: HPLC on chiral stationary phase for 4.D.

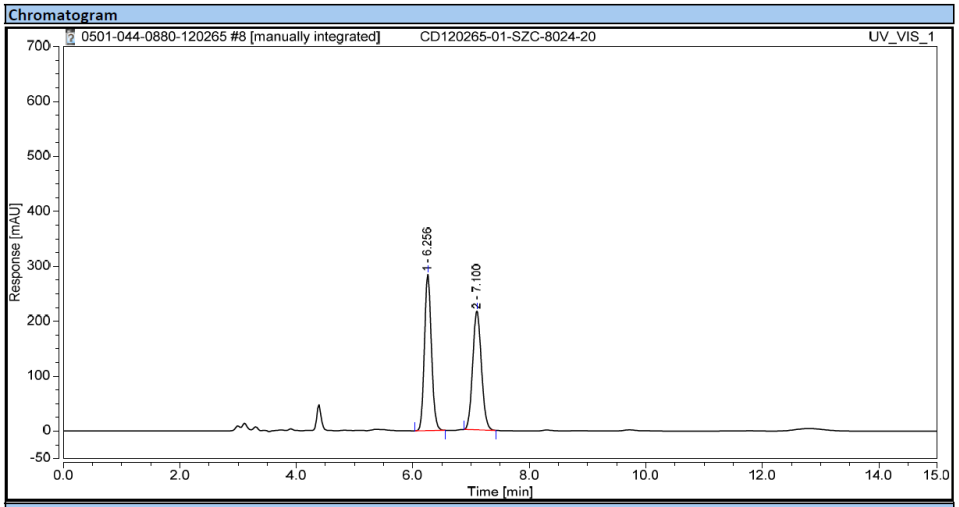

Integration Results

No.	Peak Name	Retention Time min	Area mAU*min	Height mAU	Relative Area %	Amount n.a.	Plates (EP)
1		6.256	39.373	284.590	51.1091	n.a.	13364
2		7.100	37.664	216.112	48.8909	n.a.	10607
Total:			**77.037**	**500.702**	**100.00**		

Figure S18: HPLC on chiral stationary phase for 4.E.

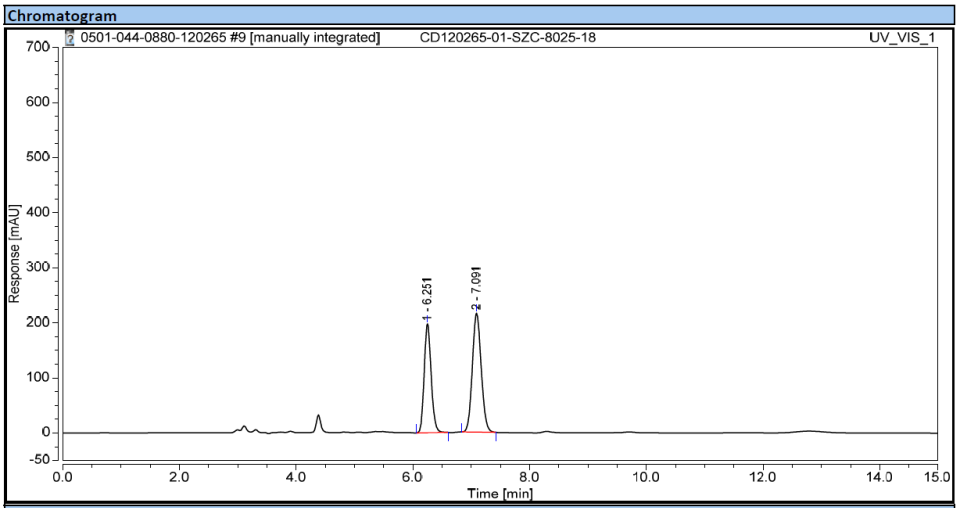

Integration Results

No.	Peak Name	Retention Time min	Area mAU*min	Height mAU	Relative Area %	Amount n.a.	Plates (EP)
1		6.251	27.249	197.683	41.8412	n.a.	13414
2		7.091	37.875	216.208	58.1588	n.a.	10532
Total:			**65.124**	**413.891**	**100.00**		

Figure S19: HPLC on chiral stationary phase for 4.F.

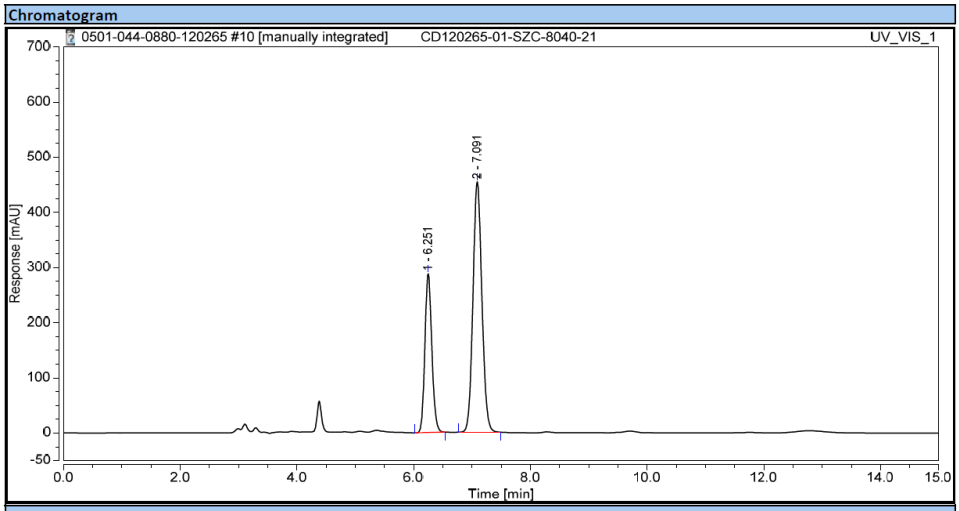

Integration Results

No.	Peak Name	Retention Time min	Area mAU*min	Height mAU	Relative Area %	Amount n.a.	Plates (EP)
1		6.251	39.529	287.929	33.0000	n.a.	13486
2		7.091	80.256	453.995	67.0000	n.a.	10456
Total:			**119.786**	**741.924**	**100.00**		

Figure S20: HPLC on chiral stationary phase for 4.G.

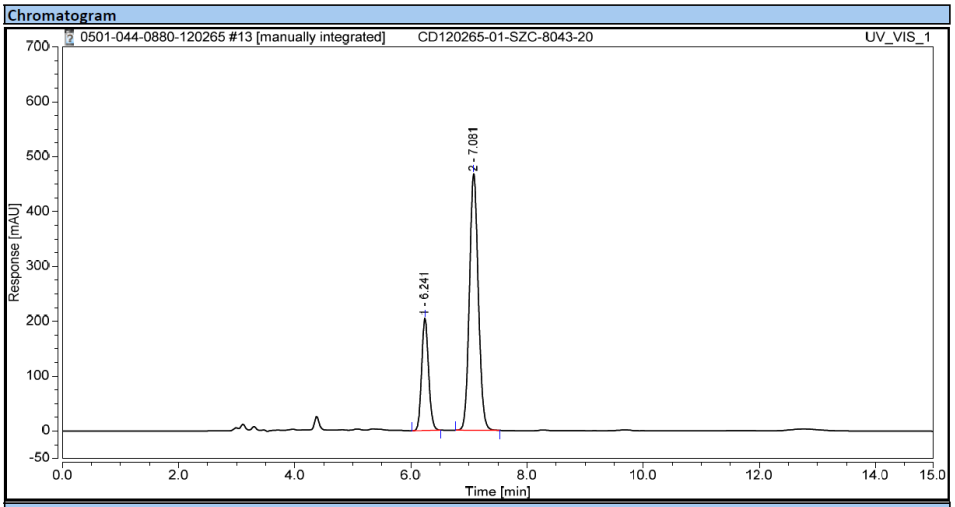

Integration Results

No.	Peak Name	Retention Time min	Area mAU*min	Height mAU	Relative Area %	Amount n.a.	Plates (EP)
1		6.241	28.160	204.945	25.4131	n.a.	13420
2		7.081	82.648	467.665	74.5869	n.a.	10432
Total:			**110.807**	**672.611**	**100.00**		

Figure S21: HPLC on chiral stationary phase for 4.H.

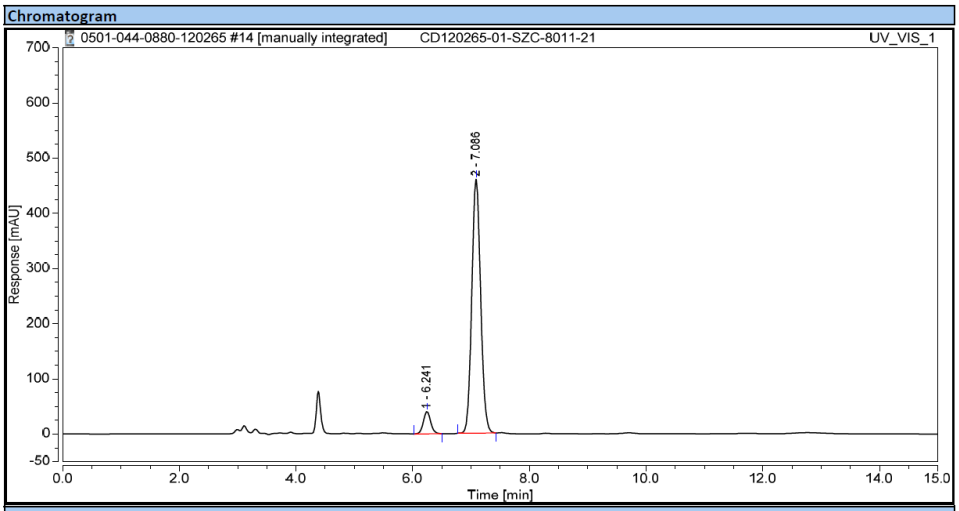

Integration Results

No.	Peak Name	Retention Time min	Area mAU*min	Height mAU	Relative Area %	Amount n.a.	Plates (EP)
1		6.241	5.841	40.514	6.7478	n.a.	12319
2		7.086	80.723	460.244	93.2522	n.a.	10519
Total:			**86.564**	**500.758**	**100.00**		

Figure S22: HPLC on chiral stationary phase for 4.I.

8. **References**

1. Chen, Gang; Gong, Wei; Zhuang, Zhe; Andrä, Michal, S.; Chen, Yan-Qiao; Hong, Xin; Yang, Yun-Fang; Liu, Tao; Houk, K., N.; Yu, Jin-Quan, *Science*, **2016**, 6303, 1023-1027.
2. Burés, J. *Angew. Chem. Int. Ed.,* **2016**, 55, 16084-16087.
3. Blackmond, D. G. *Angew. Chem. Int. Ed.,* **2005**, 44, 4302-4320.
4. Mathew, J. S.; Klussmann, M.; Iwamura, H.; Valera, F.; Futran, A.; Emanuelsson, E. A. C.; Blackmond, D. G. *J. Org. Chem*. **2006**, 71, 4711-4722.
5. Hoops S.; Sahle S.; Gauges R.; Lee C.; Pahle J.; Simus N.; Singhal M.; Xu L.; Mendes P.; Kummer U. *Bioinformatics*. **2006**, 22, 3067 – 3074.